Karaelmas Science and Engineering Journal
Journal home page: https://dergipark.org.tr/tr/pub/karaelmasfen
DOI: 10.7212/karaelmasfen.1524135

Research Article
Received / Geliş tarihi : 29.07.2024
Accepted / Kabul tarihi : 27.08.2024

Investigation of a New Blade Design to Improve the Efficiency of an Axial Fan Used in an Underground Mine

Bir Yeraltı Madeninde Kullanılan Eksenel Fanın Verimliliğini Artırmak İçin Yeni Bir Kanat Tasarımının Araştırılması

Güneyhan Taşkaya, Beytullah Erdoğan*

Zonguldak Bülent Ecevit University, Engineering Faculty, Mechanical Engineering of Department, Zonguldak, Türkiye

Abstract

The blade geometry of a 40 cm diameter axial fan with a front stator cylindrical duct used in the ventilation of an underground mine is redesigned. The Computer Aided Design (CAD) geometry of the existing fan was extracted and all parameters were analysed. Keeping the geometrical characteristics of the real fan constant, a redesign was made according to the system requirements and a new blade profile was selected to provide the required lifting force. In addition to National Advisory Committee for Aeronautics (NACA) 747A315 and NACA 6412 airfoils, Computational Fluid Dinamics (CFD) analysis of NACA 63-412 airfoil was performed and airfoil performance ratios (C_L/C_D) were determined. The rotor geometry designed using the NACA 63-412 airfoil and the existing fan geometry were combined in CAD environment. The CFD results of the new fan were compared with those of the existing fan The CFD results of the new fan were compared with the existing case. Accordingly, in the existing fan, at 3700, 4000, 4700 rpm and a constant flow rate of 2 kg/s, 25%, 37.5% and 43.5% performance increases were obtained with mass flow rates of 2.5, 2.75, 2.87 kg/s respectively in the new fan design.

Keywords: Airfoil, axial fan, CFD, fan blades, rotor, ventilation.

Öz

Bir yeraltı madeninin havalandırılmasında kullanılan 40 cm çapındaki ön statorlu silindirik kanallı eksenel fanın kanat geometrisi yeniden tasarlanmıştır. Mevcut fanın Bilgisayar Destekli Tasarım (CAD) geometrisi çıkarılmış ve tüm parametreler analiz edilmiştir. Gerçek fanın geometrik özellikleri sabit tutularak sistem gereksinimlerine göre yeniden bir tasarım yapılmış ve gerekli kaldırma kuvvetini sağlayacak yeni bir kanat profili seçilmiştir. Ulusal Havacılık Danışma Komitesi (NACA) 747A315 ve 6412 kanat profillerine ek olarak NACA 63-412 kanat profilinin Hesaplamalı Akışkanlar Dinamiği (HAD) analizi yapılmış ve kanat performans oranları (C_L/C_D) belirlenmiştir. NACA 63-412 kanat profili kullanılarak tasarlanan rotor geometrisi ile mevcut fan geometrisi CAD ortamında birleştirilmiştir. Yeni fanın CFD sonuçları mevcut fanın sonuçları ile karşılaştırılmış ve yeni fanda farklı dönüş hızlarında kütlesel debide %45'e varan bir artış sağlanmıştır. Buna göre mevcut fanda 3700, 4000, 4700 devir/dakika ve 2 kg/s sabit debide yeni fan tasarımında 2.5, 2.75, 2.87 kg/s kütle debileri ile sırasıyla %25, %37.5 ve %43.5 performans artışları elde edilmiştir.

Anahtar Kelimeler: Airfoil, eksenel fan, HAD, fan kanatları, rotor, havalandırma.

1. Introduction

Underground mining is undoubtedly very important in terms of the economic and strategic position of states and their competition with each other. Sustainable underground mining is only possible by providing favorable conditions for safe access and extraction. Safe access to the mine is largely dependent on ventilation. The evacuation of toxic gases that threaten the health and safety of workers in mines, spontaneously or during mining activities, and keeping the accumulated explosive and flammable gases at the desired amounts are provided by the ventilation system. In addition, a ventilation system is needed to disperse mine dust, to ensure the correct operation of machinery and equipment, and to control temperature and humidity to increase worker comfort. In order to fulfil all these conditions,

*Corresponding author: beytullah.erdogan@beun.edu.tr

Güneyhan Taşkaya orcid.org/0000-0003-3267-6091
Beytullah Erdoğan orcid.org/0000-0002-6120-9196

the ventilation system is expected to operate 24 hours a day. This results in a very high consumption of electrical energy. The rapid development of needs and technology has made it necessary to use limited energy resources more carefully and effectively. Less energy consumption increases environmental sustainability by reducing the carbon footprint, as well as reducing costs, enabling technological progress and enabling countries and organizations to compete with each other. Therefore, energy efficiency is a fundamental energy policy element for all countries. For this reason, considering that one third of the electricity demand of a typical mining operation is caused by the ventilation system, it is aimed to minimize the losses in the system, device and process and to obtain the same system output with less energy consumption (Panigrahi and Mishra 2014).

The necessity of high efficiency of the components used in ventilation increases the importance of studies to improve the performance of axial fans, one of the most important components of the system. Axial fans have a wide range of applications such as aircraft engines, heat exchangers, cooling of computers, heating-cooling-air conditioning installations of industrial processes, tunnel and mine ventilation and their physical properties (blade profile, number of blades, hub geometry, etc.) vary according to the needs of the application in which they are used. In underground mine ventilation, where the need for fresh air is at the forefront, directing blades that protect the fan from mine dust and at the same time distribute the air evenly can be preferred at the fan inlet, as well as at the fan outlet or at both inlet and outlet of the fan. The air coming axially to the fan gains kinetic energy during its movement on the rotor blades. The directing blades of the fan ensure that the air flow is directed uniformly towards the rotor. The efficiency of the fan depends on how much kinetic energy is generated, how low the rotor losses can be kept and how much of this kinetic energy is converted into static pressure. Therefore, the calculation of blade angles, determination of the number of blades and selection of blade profiles are very important in fan efficiency (Çakır 2018). Until recently, the effects of certain parameters such as radial distribution of Euler work, blade load, blade profile, blade tip clearance, number of blades, ratio of hub radius to tip radius of the fan on axial fan performance have been demonstrated and accordingly, axial fan efficiencies have increased. With the increase in computer speed and capacities after 1980s, Computational Fluid Dynamics (CFD) has been widely used in studies to improve the performance of axial fans. The cheap and fast CFD method has enabled the determination of the effects of new parameters on axial fan performance, which are difficult and costly to investigate by experimental methods (İlikan 2014).

Keklikoğlu (2019), developed an application code for fan design using some empirical equations in order to examine the effects of all parameters of axial fan design. The results obtained by performing experiments in the test setup prepared according to Air Movement and Control Association (AMCA) standards with the new prototype produced by making a sample design were compared with the results obtained with ANSYS-CFX software. According to the experimental and numerical results of the study, a new design code was developed for the designers as the pressure difference and volumetric flow rate values were quite close (Keklikoğlu 2019). Jung and Joo (2019) examined the effect of fan inlet core length on the efficiency of the fan in their study with the axial fan of an outdoor unit air conditioner. They determined that the vortex occurring at the edge of the fan hub inlet affects the attack edge of the blade and causes yield loss. If the input core length is shorter than a certain value, the loss increases, but the rounded corner shape improves the situation. The results showed that the efficiency increases at certain inlet hub length due to the interaction between the hub vortex and the blade (Jung and Joo 2019). İlikan (2014), investigated the effects of airfoil arrangement patterns on fan performance and three-dimensional flow structure. When the results of the CFD solutions made with the frozen rotor approach are compared with the experimental results, no significant changes are observed in the performance values, but differences are observed in the design flow rates. It is observed that shifting the fan blades backwards reduces the total pressure and efficiency of the fan at low flow rates, while it has no effect at design flow rates and high flow rates. The main novelty of this study is the demonstration that the unstable region in the performance curve of axial fans is completely eliminated by the application of positive translation to the fan blades, and thus the stable operating region is significantly expanded (İlikan 2014). Çakır (2018), carried out two-stage CFD studies with stator axial fan. In the first stage of the study, the effects of rotor-stator interaction surface models on fan performance were compared. At a single rotational speed, the static pressure and flow rate values were closer to each other in the stationary impeller and mixing surface models, but remained lower than the experimental results. It was observed that the time transformation method was closer to the experimental results. In the second stage of the study, two different models were created by applying 300 shifts to

the rotor airfoils forward and backward in the chord direction. In a study using a mixing surface model, it was concluded that forward shifting relatively increases fan efficiency compared to rearward shifting (Çakır 2018). Park et al. (2019), investigated the effect of reducing tip leakage flows on the efficiency of an axial flow fan used in an air conditioning outdoor unit. They aimed to prevent tip leakage flows and related vortices by coating the casing of the axial fan. With a CFD study at 154.000 Reynolds number, they concluded that reducing tip leakage flows increases efficiency by reducing total pressure loss (Park et al. 2019). Galpin et al. (2017) compared the total pressure and efficiency results obtained from time-independent and time-dependent CFD analyses with experimental results using a single-stage transonic compressor with 20 rotor and 43 stator blades. Mixing surface model was used for time independent solution and time transform model was used for time dependent solution. In order to understand the uncertainties of the flow in advance and to establish a solution system, they first analyzed the flow on the rotor. They found that the mixing surface model gives results almost as consistent as the time transformation and that the gain is not so good compared to the mixing surface when the cost of the time transformation method is considered (Galpin et al 2017). Tonello et al. (2017), performed time-independent CFD analyses on the Franscis-99 turbine using open-source software. When they compared the results obtained from the study in which they applied the k- ω (omega) Shear Stress Transport (SST) turbulence model (partial load, high load and best efficiency point) with the experimental results, they found that the mixing surface model has no advantage over the standing wheel method in predicting the flow inside the emitter and the general characteristics of the turbine. When the rotor-stator interactions where the losses are intense are examined, it is argued that the mixing surface will be more effective, this is due to the lack of rotor-stator interaction in the emitter (Tonello et al. 2017). Castegnaro (2017) worked on the design of low-speed axial fans in which three important parameters (blade profile, stiffness ratio and insertion angle) provide the required pressure difference with the highest efficiency. He stated that there are methodological differences between traditional blade design methods of axial fans and that these differences are caused by these three parameters. Three different rotors with a diameter of 315 mm were used in the study. In one of the models, British airfoil C4 and American airfoil NACA 65 series fans were compared by considering the angle of insertion. The second study was carried out according to the stiffness distribution and the third according to the Reynolds numbers. According to the results of the study, it was stated that C4 airfoil showed higher performance than NACA 65 airfoils and C4 airfoil is the most ideal airfoil in axial fan applications (Castegnaro 2017). When designing the airfoils of turbomachinery and aircraft, it is of great importance to increase efficiency in the application. Blade efficiency is highly dependent on the on-wing flows. A high wing performance ratio, characterized by a high lift coefficient and low drag coefficient ratio, contributes to increased efficiency. Çoban (2019), conducted a CFD study with new geometries obtained by changing the geometric properties of the NACA 0018 airfoil in order to increase the performance ratio (C_L/C_D) in wings, and compared the wing performances with experimental results. Of the 3 geometries used, the first is a 165 mm long standard NACA 0018, the second is a new profile derived from NACA 0018 with a gap cut into the upper surface, and the third is another NACA 0018 wing variation with 66% of the trailing edge cut off at the vet length. Reynolds number between 20.000 - 100.000 and angle of attack between 0°-15° values. As a result, the streamlines and pressure contours of the airfoils were visually compared at the same Reynolds number at different angles of attack and at different Reynolds numbers, at the same angle of attack. The lift coefficient (C_L), resistance coefficient (C_D) and the ratio of lift coefficient to resistance coefficient (C_L/C_D) between airfoils and between different airfoils are given in the study. According to the results of the study, opening steps and gaps on the airfoil affected the flow, but this effect was not favorable in the lift coefficient compared to the standard airfoil geometry. In addition, the hollow model performed better than the stepped model, and it was found that the drag coefficient performance decreased while the lift coefficient performance increased in all models as the Reynolds numbers increased (Çoban 2019). Dilmaç (2019), conducted a series of analyses to prove that the performance of wind turbines can be improved by thickening the trailing edge of the airfoil geometry symmetrically and asymmetrically and at certain rates. As a result of the aerodynamic analyses, the aerodynamic performance of the NACA 4415 airfoil at 10° angle of attack was increased by 5% by thickening the airfoil by 2% just below the vet exit edge. After determining the optimum thickness, 2D analyses were performed at Re=124.000 at angles of attack between 00-180, and as a result, the C_L coefficient of the new variation was better, while the C_D coefficient was close in both profiles. By applying 3D CFD analysis to 2 geometries with a rotor diameter of 1,44 m, which he produced and

tested in the wind tunnel, he obtained 4,42 Nm torque with NACA 4415 and 5,12 Nm torque with the second thickened variation (Dilmaç 2019) Korkmaz (2018), suggested that changing the airfoil shape increases the efficiency by delaying flow separation at different speeds and angles of attack. According to the results of CFD analyses of NACA 4412 and NACA 63-215 profiles with 2 new profiles obtained by changing the x/c ratio (the ratio of the distance of the maximum blade thickness point from the edge of attack to the length of the vet), it was seen that the new airfoils increased the maximum performance ratio. Thus, by delaying the flow separation between 2-4 degrees, it was able to postpone the stall due to the sudden decrease in the lift coefficient (Korkmaz 2018). Bacak (2016), obtained characteristic and performance curves from CFD analyses of an axial fan and determined the optimum operating range of the fan. He compared these results with the results obtained from Wing Fan's test bench built according to AMCA 210 standard. The maximum allowable angle of attack was verified by analyzing the velocity profile around the airfoil of an axial fan (Bacak 2016). Fan et al. (2020), investigated the effects of rotation, displacement and translation methods applied to the fan blades on the aerodynamic and structural performance of the fan. The variation of the wing geometry was performed with a Free Form Deformation (FFD) approach. According to the results obtained from CFD analyses, rotation and scrolling methods are relatively more efficient on the aerodynamic performance of the fan. At different operating conditions, the effect of rotation on the efficiency did not always tend to increase. The excessive rotational effect at low flow rates caused the total pressure differential of the fan to drop sharply. According to the optimization results, rotation caused maximum stress on the wing, while the backward displacement reduced the stress on the wing surface. Up to 15% improvement in the total pressure difference was achieved with the blades formed by rotation and sliding methods (Fan et al. 2020). Bakhtar et al. (2024) has examined various add-on designs to reduce noise generated by axial fans. Their research focuses on understanding how different attachments to axial fans affect aerodynamic noise. Eight distinct design cases have been evaluated, including the extension of outlet and inlet ducts, the use of Chevron nozzles, the placement of spherical balls inside the fan in staggered and straight patterns, the application of a wavy inner wall treatment, and combinations of some of these designs. To analyze the effects of these designs on noise, CFD and acoustic analyses were conducted using Ansys Fluent 2022 R1 software. The results obtained indicate that all design modifications reduced noise levels and suggest that these designs could contribute to the development of quieter fans suitable for various environments (Bakhtar et al. 2024).

Fernando and Mudunkotuwa (2021), designed a biologically-derived modification with the aim of achieving a major reduction in fuel costs and environmental impacts by reducing frictional resistance. The experimental results of the NACA 0012 airfoil were used as a reference. They investigated four different types of modifications which are lighter than the original wing. By comparing the numerical results with experimental results, they found two bio-inspired wing shapes that are more efficient than the original wing and can be incorporated into the future aerospace industry (Fernando and Mudunkotuwa 2021). Drwiega et al. (2019) discussed current research and development projects carried out within the European project to improve the effectiveness of auxiliary ventilation in underground mines. These projects are generally studies to improve the parameters affecting the fan efficiency by modifying the rotor blades. The rotor blades and modifications used in the study were obtained by printing from 3D printing. Both aerodynamic and structural performance results were obtained by CFD and Finite Element Method (FEM) analyses on the existing and modified wings. By comparing the fan characteristic graphs before and after the modification, it was observed that the pressure difference, power and efficiency were increased in the modified fan (Drwiega et al. 2019). Fakhari and Mrad (2024), conducted an optimization study of an axial flow fan used in underground mine ventilation using the parameters of angle of attack, tip clearance, speed, hub to tip ratio and number of blades. By comparing the experimental results with the results obtained from CFD analysis, they stated that by reducing the number of blades and tip span, a performance increase of 9% was achieved and confirmed the experimental results with an error rate of less than 5% (Fakhari and Mrad 2024). NACA airfoils in order to propose an airfoil for use in underground mine ventilation fans Panigrahi and Mishra (2014), conducted CFD analyses with 6 different in 2014. By determining the lift and drag ratios of the wings at different angles of attack, the maximum aerodynamic performance ratios were compared. At 150 angles of attack, they found that the profile with the highest performance ratio was NACA 747A315. (Panigrahi and Mishra 2014). Kong et al. (2023) optimized the blade geometry of low-pressure axial flow

fans to enhance their aerodynamic performance. Traditional design theories often fall short in addressing the complexity of 3D internal flows, leading to suboptimal blade profiles and spanwise distribution. To address this, he developed a surrogate-assisted multi-objective optimization process, supported by CFD methods, to determine the optimal blade shape under two typical operating conditions. Sixteen parameters were selected, and response functions were constructed using kriging models, followed by a multi-objective genetic algorithm to identify the best solutions. The results indicate that efficiency can be improved by %1,26 under low mass flow conditions and by %5,47 under high mass flow conditions. The optimization also led to a better distribution of low-pressure zones along the blade leading edge and a reduction in tip leakage vortex intensity. This study presents a successful approach for optimizing fan blade geometry (Kong et al. 2023).

Hassen (2021), focused on developing new blade types for underground mine ventilation fans, arguing that higher efficiency can be achieved with a more uniform flow distribution. For this purpose, firstly, performance comparison studies were carried out with CFD using NACA747A315 and NACA 6412 profiles. Since it achieved higher efficiency, the NACA 6412 profile continued its studies. With the analyses performed at 30°-40° angles of attack with 4 different designs, namely fixed vane, tapered vane, skewed vane and tapered skewed vane, the flow velocity, homogeneity and efficiency of the designs were investigated. He stated that high homogeneity and efficiency do not necessarily mean high system efficiency and these two parameters should be evaluated together with system efficiency (Hassen 2021). Krasyuk and Kosykh (2023) address the aerodynamic design of axial fans by utilizing an impeller and an inlet guide vane to reverse the direction of airflow. This process involves stopping the rotation of the impeller while allowing the guide vane to rotate, aiming to enhance fan efficiency in reverse mode. The authors have developed a novel blade angle analysis method to identify airflow parameters under reversal conditions. Furthermore, they delineate the parametric regions in which the proposed reversal approach is effective. A design of a fan exhibiting similar performance curves in both forward and reverse airflow is undertaken. The swirl ratios of the flow within the guide vane are correlated with the axial velocity ratios, based on the geometrical similarity of the blade profiles of the impeller and guide vane at an average radius (Krasyuk and Kosykh 2023).

In the aforementioned literature studies to improve the performance of axial fans, some researchers have focused on the optimization of all parameters required for fan design (Keklikoğlu 2019, Bacak 2016, Fakhari and Mrad 2024) while others have focused on the airfoils, arguing that the fan efficiency is largely dependent on the flows over the blade. Axial fan performance has been improved by many studies such as the application of shifting and translation methods on airfoils (Çakır 2018, İlikan 2014, Fan et al. 2020), changing the geometric properties on the existing airfoil (Çoban 2019, Dilmaç 2019, Korkmaz 2018), Drwiega et al. 2019) comparing the performance of different airfoils (Panigrahi and Mishra 2014, Hassen 2021). However, very few of them are related to axial fans used in underground mine ventilation (Panigrahi and Mishra 2014, Fakhari and Mrad 2024, Hassen 2021) and more studies are needed in this field.

The innovative aspect of this study compared to other studies is that it contributes to energy efficiency by improving the performance of a fan used in a real mining operation, and at the same time, an alternative blade profile is presented to increase the efficiency of axial fans used in underground mine ventilation. CAD geometry of the existing fan was extracted, all parameters were analyzed and CFD analysis was performed. When the ventilation systems used in underground mining were investigated to be used in the blade design of the existing fan, NACA 747A315, NACA 6412 blades were used (Panigrahi and Mishra 2014, Hassen 2021) and blade performance comparison studies of NACA 63-412 blades were carried out as an alternative to these blades. The mass flow rates of the polluted air drawn from the mine at different speeds and at the same pressure difference values of the new fan created with the alternative blade with the highest blade performance ratio were compared. In this study, the blade geometry of the pre-stator cylindrical ducted axial fan used in the ventilation of an underground mining operation in Zonguldak Mining Basin was redesigned due to low efficiency.

2. Material and Methods

Axial fans used in underground mine ventilation have stator blades to distribute the air evenly and these blades can be preferred in front of the rotor to protect the fan from the adverse conditions of the mine environment (Çengel and Cimbala 2018). The air coming to the fan in axial direction is directed towards the rotor blades by the stator blades and its pressure is increased by being compressed by the rotor

blades. Thus, the air is displaced in the desired direction. The axial fan whose specifications are given in Table 1 is used in the ventilation of a real mine operation.

Table 1. Technical and geometrical characteristics of the existing fan with Ø400 mm used in the mine.

Parameter	Property
Weight and Power	60 kg and 9 HP
Air Pipe Diameter	400 mm
Operating Pressure	4-6 bar
Air Output Speed	15 m/s
Volumetric Flow	143 m^3/min
Air Consumption at Normal Pressure	175 m^3/min
Number of Revolution	3700 - 4700 rpm
Pressing Height	20 mmwc (milimeter water column)
Hub Diameter	200 mm
Number of Rotor Blades	6 pieces
Number of Stator Blades	6 pieces

In order to increase the efficiency of the fan, firstly, all design parameters of the fan were reviewed by applying the classical axial fan design method. Considering the design conditions specified in the fan catalogue, lift coefficients and drag coefficients were determined according to the stiffness values calculated for the hub end and middle layers of the blade (Keklikoğlu 2019). The rotor blades of the fan rotate with the flywheel around it and there is no blade end gap (Figure 1). Certain parameters such as fan diameter, hub-tip ratio, number of blades, blade angle, vet length were found to be suitable for the design and it was decided to redesign the blade geometry by selecting a new blade profile.

2.1. Analytical Approach

The methods and techniques applied should be given in an understandable way. It should be supported by previous references. Statistical models and methods of analysis should be clearly stated.

Air enters the airfoil at the attack edge and leaves the wing at the trailing edge (Figure 2). The hump part of the airfoil is referred to as the low-pressure zone or suction edge, and

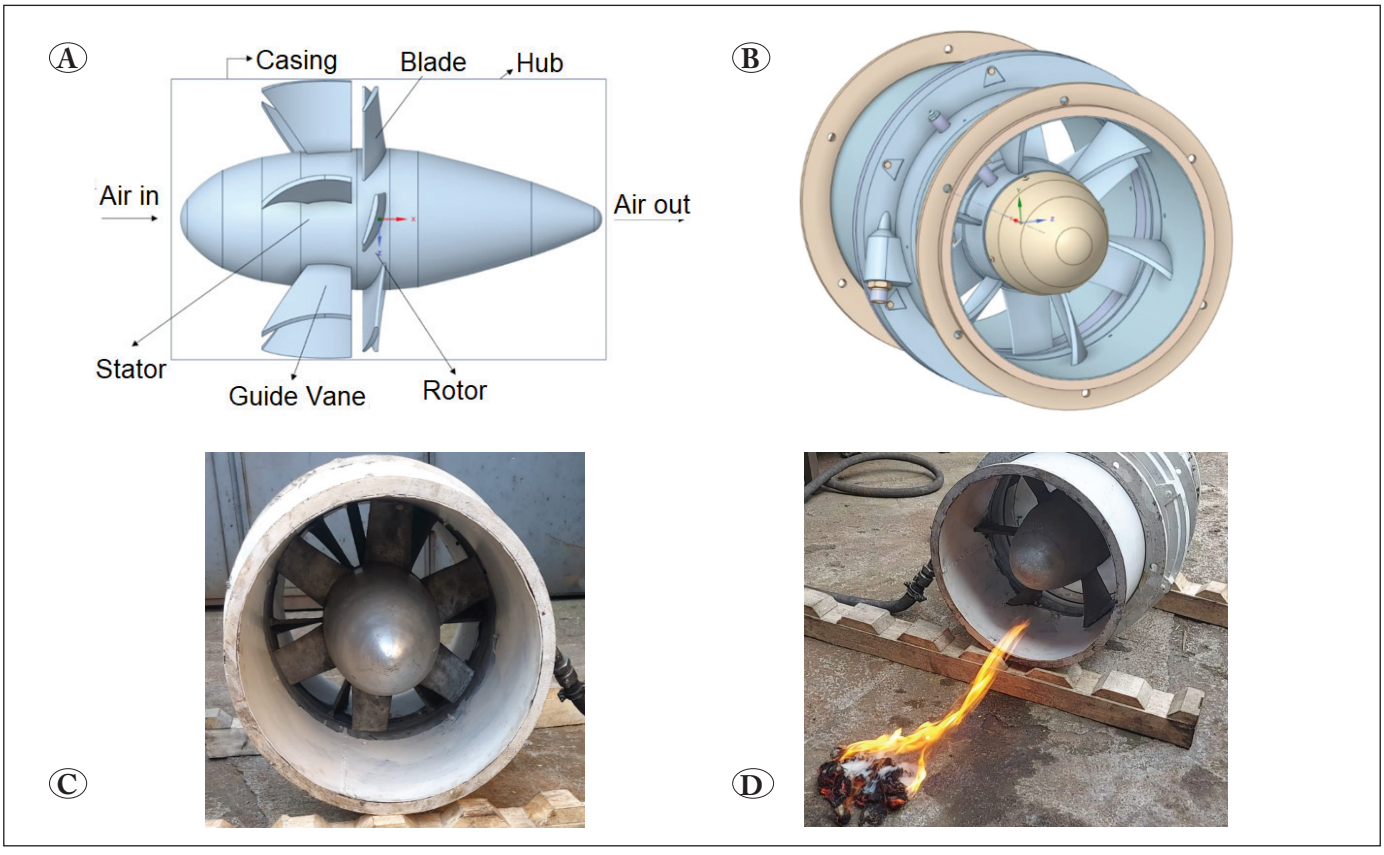

Figure 1. Side view **(A)** and isometric view **(B)** of the fan created by software, real fan image **(C)** and the flow direction **(D)** of the fan used in the underground mine.

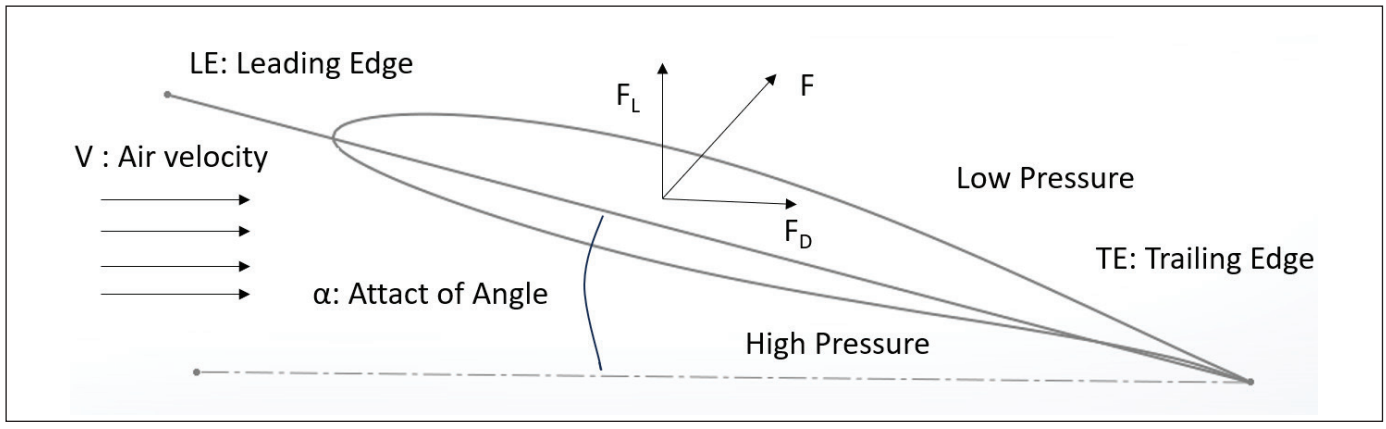

Figure 2. Forces acting on the airfoil (Yılmaz et al. 2018).

the hollow part is referred to as the high pressure zone or compression edge. The angle between the direction of arrival of the air to the wing and the wing is called the angle of attack. The lift coefficient increases until the optimum value of the angle of attack. When the angle of attack reaches a certain value, the lift coefficient becomes maximum and starts to decrease rapidly after this value. The fan switches to unstable operation. This condition can also be expressed as stopping the fan. In order to prevent unstable operation in fans, it is necessary to determine at which value of the angle of attack the lift coefficient reaches its maximum value and the angle of attack should be kept below this value (İlikan 2014, Köse 2018).

The high lift airfoil blades provide an increase in static pressure, while the low drag force (F_D) helps to achieve lower power consumption, thus increasing fan efficiency. Therefore, in the selection of the airfoil, it is not sufficient only to have high lift coefficients of the wings. Drag coefficients should also be low. The ratio of the lift coefficient of an airfoil to the drag coefficient (C_L/C_D) is called the airfoil performance ratio and when comparing airfoils, the airfoil with the maximum performance ratio represents the highest efficiency. C_L and C_D are given by equation (1) and (2) (İlikan 2014, Keklikoğlu 2019).

$$C_L = \frac{F_L}{0,5\rho V^2 A} \quad (1)$$

$$C_D = \frac{F_D}{0,5\rho V^2 A} \quad (2)$$

F_L: Buoyancy force (N)

ρ: Density (kg/m^3)

V: Velocity (m/s)

A: Wing projection area (m^2)

F_D: Drag force (N)

When designing axial fans, a preliminary design process is initiated and the design approach is determined by using the desired results as initial parameters (flow rate (Q, m^3/s), total pressure difference (ΔP, Pa) and speed (n, rpm)) (İlikan 2014). For this, the solidity value of the blade is needed. The solidity value (is given by equation (3).

$$\sigma = \frac{c}{s} \quad (3)$$

c: Chord distance (m)

s: Pitch distance (m)

Here "c" is the vet length (m) and refers to the distance between the LE (air's leading edge of the wing) end and the TE (the trailing edge of the wing where the air leaves) end of the wing. The distance "s", which is the distance between the two wings, is called the pitch distance (m).

Solidity value (σ) is an important parameter that determines the design approach in axial fans. When the solidty value is below 0,7, the isolated blade approach is used, when it is above 1 (one), the stepped blade approach is used, and for values in between, the mixed approach, which is a combination of both isolated and stepped approaches, is preferred (Castegnaro 2017). In the isolated blade approach, the interaction of the pressure fields of the blades with each other is ignored. In the stepped approach, the actual lift coefficient starts to change as the solidity value increases and this cannot be ignored because it reduces the fan efficiency (Keklikoğlu 2019).

Axial are designed by the classical method (İlikan 2014, Keklikoğlu 2019, Fakhari and Mrad 2024). The number

of graphs and equations used in the method is quite large. The axial fan geometry varies according to the needs of the system in which the fan will be used. In this part of the study, the methodology of the parts specific to the front stator axial fan is mainly included. Inlet and outlet vector analyses and inlet and outlet velocity triangles of front stator axial fans are given in Figure 3. The inlet and outlet angles of the stator are expressed as α_1 and α_2.

$$V_\alpha = \frac{Q}{A} \quad (4)$$

Q: Flow rate (m^3/s).

A: Cross-sectional area perpendicular to the flow direction (m^2).

Where is the vertical cross-sectional area through which the flow passes, "V_a" is the axial velocity (m/s).

In the Figure 3, "U" is the tangential velocity (m/s), "w" is the angular velocity (rad/s) and "r" is the radius of the fan (m). The relative speed "W" (m/s) is equal to the difference between the absolute speed and the tangential speed. "V_{2u}" is the tangential component of the absolute speed at the rotor inlet and is an important parameter that determines the inlet blade angle (β_1) given by equation (6) (Köse 2018).

$$U = w.r = \frac{\pi.D.n}{60} \quad (5)$$

U: Tangential velocity (m/s)

w: Anguler velocity (rad/s)

r: Radius (m)

D: Diameter (m)

n: Revolutions per minute (rpm)

$$\tan\beta_1 = \frac{U + V_{2u}}{V_a} \quad (6)$$

$V_{2u:}$ The tangential component of the absolute speed at the rotor inlet (m/s)

V_a : Axial velocity (m/s)

If the output blade angle β_2 (0) at the output edge of the rotor is β_2 (0), it is expressed as in equation (7).

$$\tan\beta_2 = \frac{U}{V_a} \quad (7)$$

U: Tangential velocity (m/s)

V_a : Axial velocity (m/s)

The relative flow velocities (W_1 and W_2) at the inlet and outlet of the rotor are given in equations (8) and (9).

$$W_1 = \frac{V_a}{\cos\beta_1} \quad (8)$$

$$W_2 = \frac{V_a}{\cos\beta_2} \quad (9)$$

V_a : Axial velocity (m/s)

The average blade angles and average relative flow velocities at the inlet and outlet of the rotor are given by equations (10) and (11).

$$\tan\beta_m = \frac{\tan\beta_1 + \tan\beta_2}{2} \quad (10)$$

β_1: Wing entry angle

β_2: Wing exit angle

$$W_m = \frac{V_a}{\cos\beta_m} \quad (11)$$

β_m: Avarege wing angle

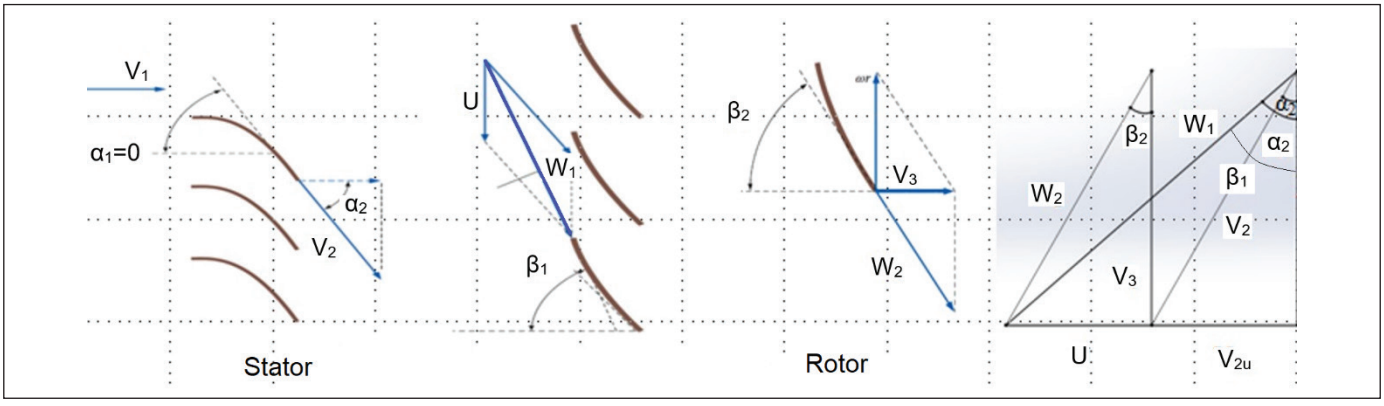

Figure 3. Vector analysis and speed triangles of axial fans with front stator (Çengel and Cimbala 2018).

W_m : Average relative flow velocity (m/s)

V_a : Axial velocity (m/s)

The useful power is the product of the flow rate of the fan and the total pressure difference as given by equation (12) and its unit is Watt. The delivered power is equal to the product of torque and angular velocity as expressed by equation (13).

$$W_{hydraulic\ power} = Q.\Delta P_t \quad (12)$$

ΔP_t: Total pressure differance (Pa)

$$W_{shaftpower} = w.\tau \quad (13)$$

τ: Torque (Nm)

w: Anguler velocity (rad/s)

In axial fans, the tangential velocities at inlet and outlet are equal and the shaft power can be calculated directly from equation (14). Here "$\dot{m}$" is the mass flow rate (kg/s).

$$W_{shaft\ power} = \dot{m}.U.V_{2u} \quad (14)$$

$\dot{m}$: Mass flow rate (kg/s)

U: Tangential velocity (m/s)

V_{2u}: The tangential component of the absolute speed at the rotor inlet (m/s)

The efficiency of axial fans (η) is defined as the ratio of the useful load to the delivered power as given by equation (15) (Çengel and Cimbala 2018).

$$\eta = \frac{Q.\Delta P_t}{\dot{m}.U.V_{2u}} \quad (15)$$

Q: Flow rate (m^3/s)

ΔPt: Total pressure differance (Pa)

$\dot{m}$: Mass flow rate (kg/s)

U: Tangential velocity (m/s)

V_{2u}: The tangential component of the absolute speed at the rotor inlet (m/s)

2.2. Numerical Approach

In recent years, numerical methods have been used more and more compared to experimental methods because they are more economical and save time. With the computational fluid dynamics method, it is possible to quickly simulate complex geometries and systems.

Here the solution of two equations characterizing the flow is needed. One of them is the continuity equation expressing the conservation of mass (16) and the other is the Navier-Stokes equation derived from Newton's law of motion (17).

$$\frac{\partial \rho}{\partial t} + \frac{\partial}{\partial x_i}(\rho u_i) = 0 \quad (16)$$

$$\frac{\partial}{\partial t}(\rho u_i) + \frac{\partial}{\partial t_i}(\rho u j u_i) = -\frac{\partial p}{\partial x_i} + \frac{\partial}{\partial x_j}\left(\mu_{eff}\left(\frac{\partial u_i}{\partial x_j} + \frac{\partial u_i}{\partial x_i}\right)\right) + Su_i \quad (17)$$

P: Pressure (Pa)

μ: Dynamic viscosity (Pa.s)

t: Time (s)

u: Velocity vector (m/s)

i: The velocity component of the physical quantity in the x direction in the Cartesian coordinate system (m/)

j: The velocity component of the physical quantity in the x direction in the Cartesian coordinate system (m/s)

r: Density (kg/m^3)

p: Pressure (Pa)

x: Position vector (m)

S: Discretisation term

In Equation 16, t is the time, u is the velocity vector and x is the position vector. The lower index i represents the velocity component of the physical quantity in the Cartesian coordinate system. In Equation 17, P represents pressure and μ represents dynamic viscosity. A source term is added to the momentum equation, denoted by the mass forces (e.g. gravitational force), S.

In this study was carried out with ANSYS Fluent 2022 R1 software, which uses the finite volume method as a discretization method. With this software, which allows to determine the fluid dynamic forces and pressure distribution acting on the airfoil, firstly a validation study was carried out and then 3D CFD analyses of NACA 747A315, NACA 6412 and NACA 63-412 airfoils were performed and airfoil performance ratios were determined. The blade with the highest blade performance ratio was compared with the flow rate and pressure difference results determined by the analyses of the existing fan geometry.

2.2.1. Validation Study

For the validation study, a study was selected from the literature in which the performance ratio comparison was performed by 3D CFD analysis of airfoils (Fernando and

Mudunkotuwa 2021). In this study, a validation study comparing the experimental results of NACA 0012 with the results of CFD analysis is taken as a reference. The analysis geometry was obtained by taking the NACA 0012 airfoil profile coordinates from the Airfoil Tools official website and using the Design Modular CAD programme in the ANSYS Fluent interface (Yılmaz et al. 2018). As boundary condition, velocity inlet is modelled as velocity inlet 30 m/s, total pressure at the outlet is "0" Pa and wing surface is modelled as wall boundary condition Figure 4(a). The mesh structure of the analysis geometry was created using ANSYS Meshing. For the precise solution of the boundary layer on the wing surface, the thickness of the first cell was chosen to be y+ <1 and the k-ω SST turbulence model was used as the turbulence model (Luo et al. 2017). The number of elements used was kept around 1 million by adhering to the study. The network structure is given in Figure 4(b).

The graph of the C_D values obtained by CFD analysis and the C_D values obtained by experimental results are given in Figure 5.

Table 2 shows the C_L and C_D values obtained experimentally and numerically at different angle of attack values. As a result of the verification study, it is seen that similar results are obtained with the reference study (Figure 6). The reference study (Fernando and Mudunkotuwa 2021) for validation

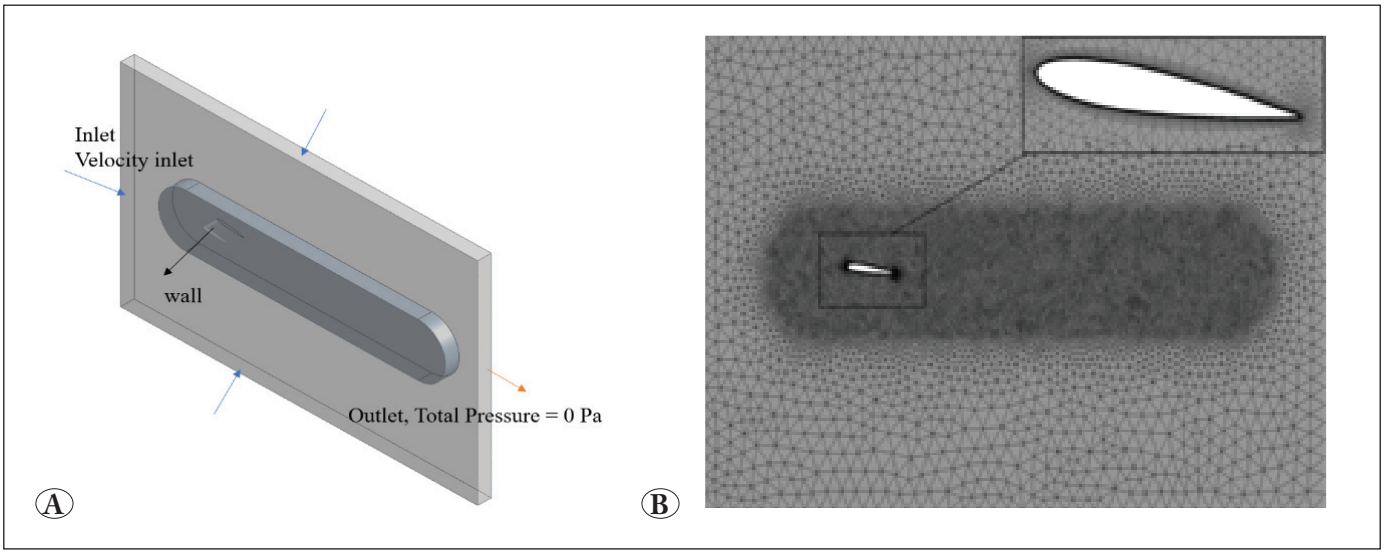

Figure 4. Mathematical representation of boundary condition **(A)**, Network structure of the verification analysis geometry at 7° attack angle (B).

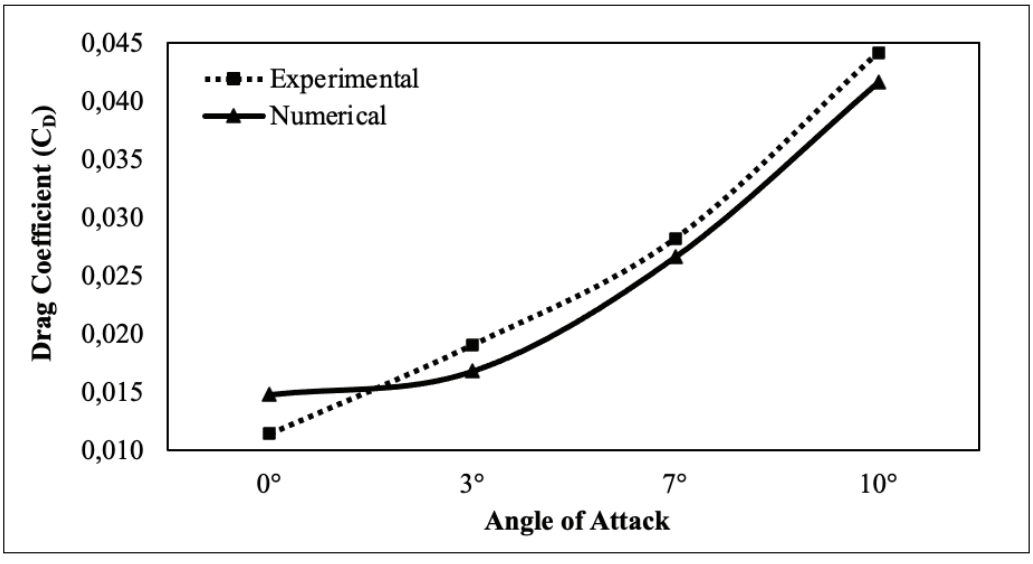

Figure 5. CFD analysis result comparison graph of the validation study with experimental results.

Table 2. Validation results of the NACA 0012 3D.

Angle of Attack	Experimental Results		Numerical Results		Error (%)			
	Lift Coeff. (C_L)	Drag Coeff. (C_D)	Lift Coeff. (C_L)	Drag Coeff. (C_D)	Lift Coeff. (C_L)	Drag Coeff. (C_D)	Lift Coeff. (C_{Lref})	Drag Coeff. (C_{Dref})
0°	-0.0039	0.0114	-0.0031	0.0147	20.63	29.23	15.43	61.18
3°	0.4619	0.0190	0.3011	0.0167	34.82	12.03	34.38	8.15
7°	0.6677	0.0282	0.6751	0.0265	1.12	5.73	5.10	11.60
10°	0.8220	0.0441	0.9350	0.0415	13.75	5.86	17.46	6.43

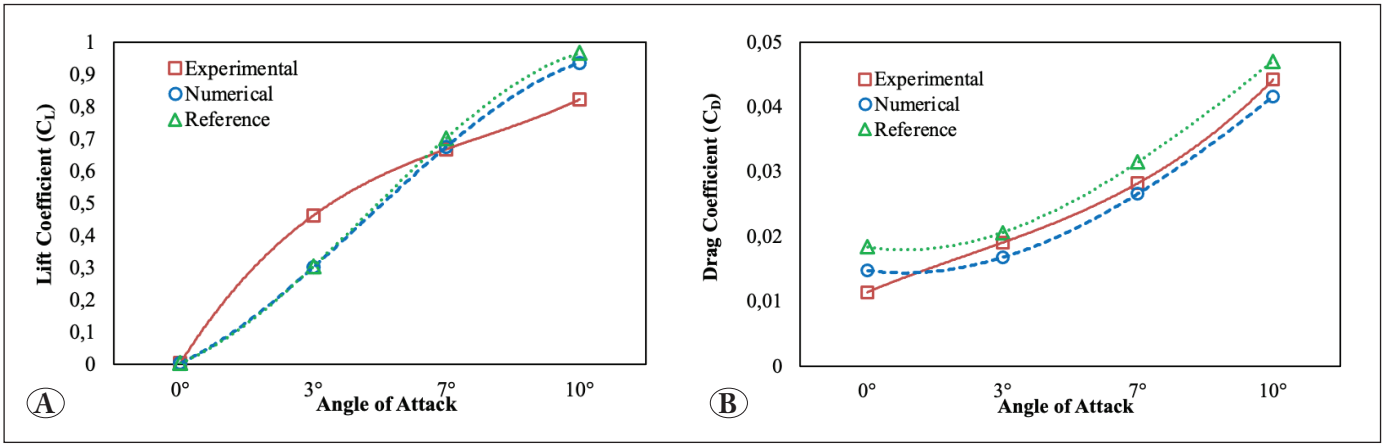

Figure 6. CFD analysis result comparison graph of experimental, numerical and reference studies **A)** Lift coefficient (C_L) comparison. **B)** Drag coefficient (C_D) comparison.

converges to the experimental values with a large error rate. In our study, convergence was obtained with similar error rates. However, the authors of reference study reached acceptable error rates (5%-10%) with 7° angle of attack and they continued their study with 7° angle of attack. It can be clearly seen that our error rate at 7°is lower than the reference study.

2.2.1. CFD Analysis

In this study, in order to propose a new blade profile as an alternative to the two blade profiles proposed in the literature for underground mine fans to be used in the blade design of the axial fan currently used in the underground mine, 3D CDF analyses of the profiles were performed and C_L/C_D values were compared. After transferring the coordinates of the airfoils to the Desing Modular, a 3D airfoil geometry was obtained by creating a surface and giving depth. In the validation study, the flow volume was obtained by giving depth to the flow area formed around the airfoil in accordance with the flow volume geometry used as a reference. In over-wing flows, the flow characteristics change abruptly on and around the wing surface. In order to accurately observe the effects of flow separation, especially at the trailing edge, a more precise solution should be provided in these areas. For this purpose, a body of influence (boi) geometry is added around the wing geometry up to a certain distance. Thus, the flow volume is prepared in a structure that is denser around the airfoil and becomes sparser as it moves away from the airfoil.

The mesh structure was obtained using Fluent Meshing, which allows to obtain much higher quality mesh structures with the same or less number of elements. In order to better analyze the flow variations on the wing surface and near the surface, a boi geometry was created around the wing (Figure 7). In order to solve the boundary layer around the airfoil correctly, the height of the first cell was determined as $6x10^{-6}$ m to fulfil the condition y+ < 1 and 15 prismatic layers were built on the boundary layer. For each profile, the optimum number of meshes was determined by performing an independence study from the mesh structure as coarse, medium and fine at a fixed attack angle (Figure 8). The DELL Precision 7670 mobile workstation with 12th generation i9 processor and 32 GB RAM was used in the analysis.

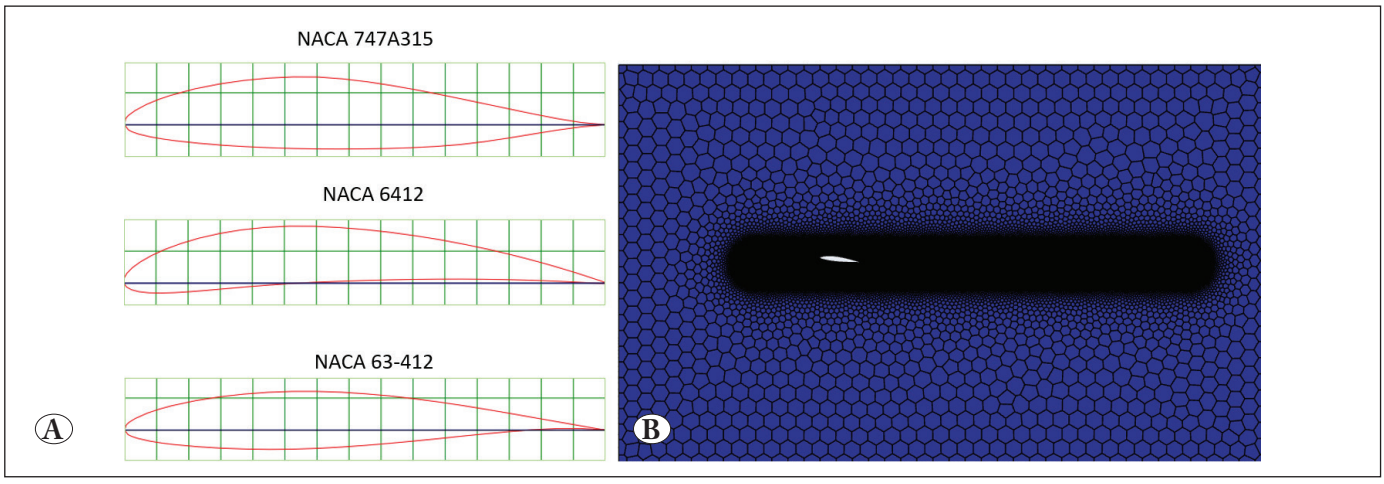

Figure 7. The airfoil shapes **(A)** and the mesh structure **(B)** of the analysis geometry for which the performance ratios are compared.

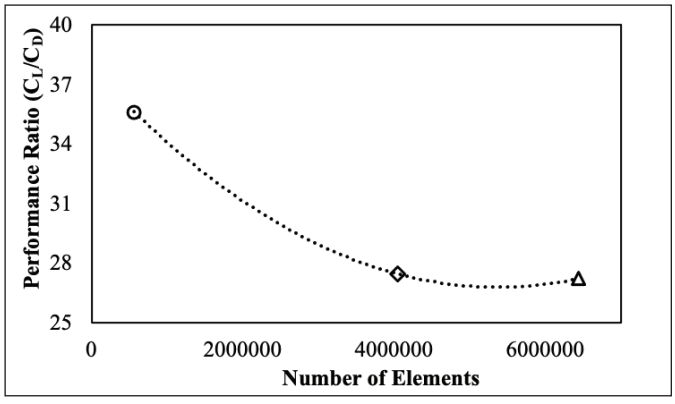

Figure 8. Optimum mesh count graph for NACA 63-412 airfoil.

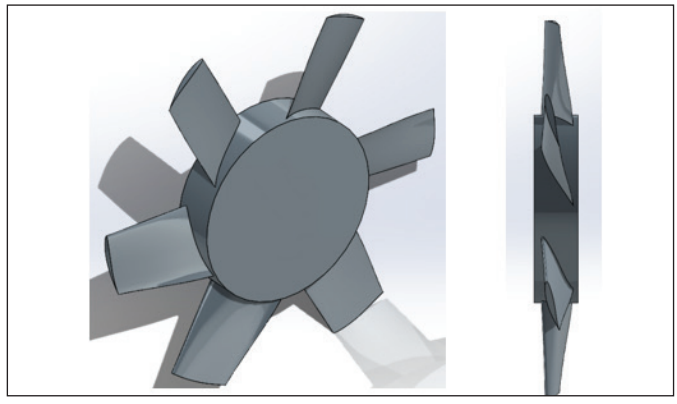

Figure 9. New wing design created with NACA 63-412, isometric view (left) and side view (right).

The analysis is performed in a time-independent manner, as is commonly done in literature studies (Çakır 2018, İlikan 2014, Keklikoğlu 2019, Galpin et al.2017, Tonello et al 2017). A k-ω SST turbulence model is chosen to provide a precise solution of the flow separation. Air of constant density (ρ=1,225 kg/m^3, μ=1,8853x10-^{5} Pa.s) was used as the fluid. The fluid velocity is 30 m/s and the analysis is performed parametrically at different angles of attack (1°, 3°, 5°, 7°, 9°, 11°). As boundary conditions, velocity inlet boundary condition, total pressure outlet boundary condition and wall boundary condition were applied. After selecting the blade profile with the highest performance, the new blade geometry (Figure 9), which was designed by taking into account the geometric features of the existing fan, was assembled to the existing fan in CAD environment and CFD analyses were performed.

The fan flow volume geometry is composed of 4 parts: inlet, stator, rotor and outlet. The rotor volume is modelled as rotating and the other volumes are modelled as stationary volumes. In axial fan analysis, Multiple Reference Frame (MRF) method is used to model rotating and stationary volumes (İlikan 2014, Keklikoğlu 2019). The modelling of the rotor and stator interface in the fan considered as a reference is done by the frozen rotor method since this study is a comparison study (Çakır 2018). The analysis conditions are provided in Table 3.

The mesh structure was created in the Fluent Meshing interface. For both fans, solutions were made independent of the network by solving in different network structures as coarse, medium, fine. In the network structure, poly hexcore elements are preferred, which allow the creation of high quality network geometry. Smooth boundary layer definition was used on the wall surfaces (Figure 10). The minimum orthogonal quality value of the network structure using approximately 8 million elements is 0,3, the maximum

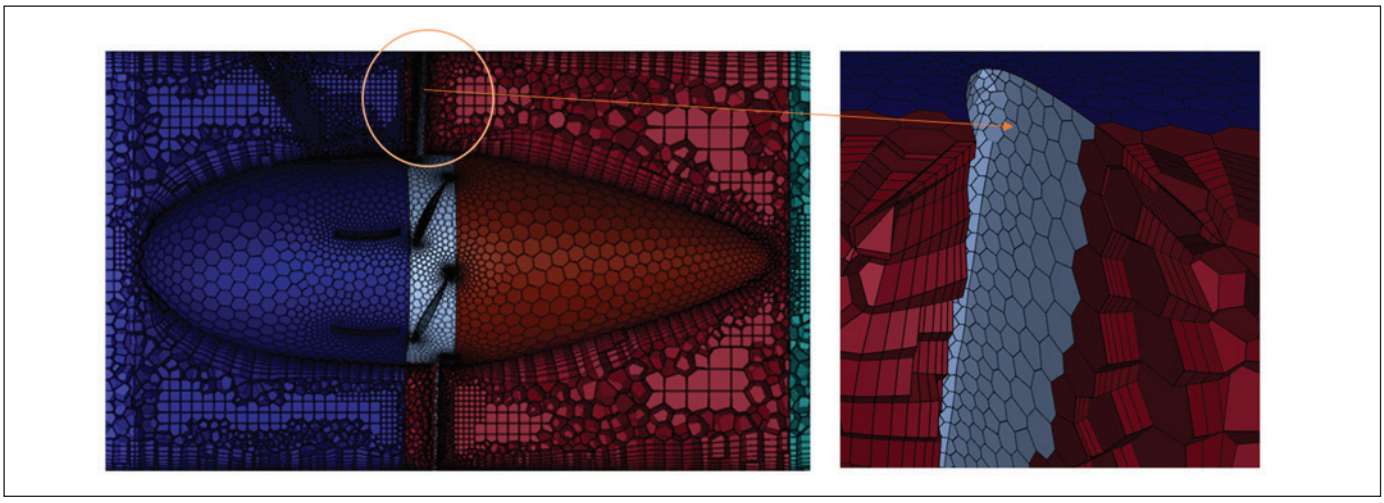

Figure 10. Fluent meshing of the new fan and a close-up view of the boundary layer around the blade.

Table 3. Analysis conditions.

General	Pressure Based, Steady
Model	k-ω SST, Production Limiter
Material	20 °C air, ρ=1,204 kg/m^3, μ=1,825x10^{-5} kg/m.s
Cell Zone Condition	MRF, Frozen Rotor, Rotating-Domain, 4000 rpm
Boundary Condition	Inlet: Mass Flow 2 kg/s, Outlet: 0 Pa
Method	Coupled, Second Order

aspect ratio value is 56 and the maximum skewness value is 0.7.

When Figure 10 is analyzed, it is seen that the maximum performance ratios of NACA 6412 and NACA 63-412 airfoils are reached at 3° attack angle. The NACA 747A315 airfoil reaches maximum performance at 5° angle of attack, but its performance at this angle of attack is lower than the other two airfoils.

3. Results and Discussion

This section is presented in two stages. The Stage 1 includes the results of the performance ratio comparison studies between the airfoils for the blade design of the existing fan. Stage 2 includes the results of the comparison of the CFD analyses of the new fan geometry and the existing fan geometry obtained by mounting the new blade designed with the blade profile with the highest performance among the blade profiles we tested to the existing fan in CAD environment.

3.1. Wing Profile Performance Ratio Comparison Study

After determining the lift coefficient required by the system (Table 4), it is crucial to correctly select the airfoil that will provide this lift coefficient. All 3 airfoils provide the lift coefficient required by the system. However, which one will perform better in the system is determined by the blade performance ratio.

With 3 different wing geometries NACA 747A315, NACA 6412 and NACA 63-412, C_L and C_D values were calculated at 6 different angles of attack (α=1-11°) and C_L/C_D ratios are given in Table 5. As a result of the CFD analyses performed with these airfoils, it was found that the airfoil performance ratio of NACA 6412 was higher than the NACA 747A315 airfoil, and the NACA 63-412 airfoil had the highest performance ratio.

The performance ratios of the airfoils are given in Figure 11. In the first stages of this study, the performance analysis of the existing fan airfoil and the NACA 747A315 airfoil was compared by CFD and found to be very close to each other. In the second stage of the study, airfoils with higher performance ratios were investigated, and there was no need to compare with the existing airfoil due to the information obtained from the first stage.

The distribution of the velocity vectors of the airfoils at an angle of attack of 7°, the velocity profiles around the airfoils (left) and the velocity contours (right) are shown in Figure 12. A uniformly distributed velocity profile is observed on the surface of the blades. Looking at the trailing edge of the profiles, NACA 63-412 is the profile where the flow separation starts the latest. Looking at the C_L graphs of the

Table 4. The stiffness value of the system and the theoretical lift coefficient calculated according to the velocity triangles.

Airfoil	Solidity (σ)	Absolute Speed (V_{2u}) (m/s)	Entry Wing Angle (β_1)	Exit Wing Angle (β_2)	Avrg. Wing Angle (β_m)	Entry Rel. Flow Vel. ($W_{1)}$ (m/s)	Exit Rel. Flow Vel. ($W_{1)}$ (m/s)	Avrg. Rel. Flow Vel ($W_{1)}$ (m/s)	Lift Coeff. (C_L)
Hub	0.84	26.25	78.03	71.36	75.36	72.06	46.93	59.21	0.99
Mid	0.49	17.50	79.90	77.33	78.72	85.20	68.38	76.40	0.82
Tip	0.34	13.13	81.64	80.43	81.03	102.66	90.20	95.80	0.60

Table 5. Performance ratio results of airfoils.

Attack Angle	NACA 6412	NACA 747A315	NACA 63-412
	Performance Ratio (C_L/C_D)	Performance Ratio (C_L/C_D)	Performance Ratio (C_L/C_D)
1°	30.30	15.00	24.95
3°	30.93	22.94	31.61
5°	28.93	26.36	31.51
7°	23.92	24.15	27.45
9°	21.03	18.99	23.42
11°	14.75	12.98	14.86

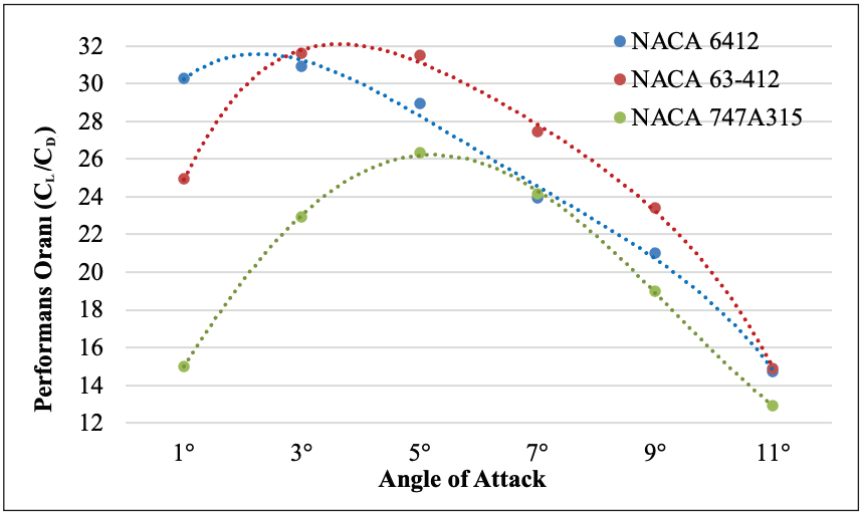

Figure 11. Performance ratio comparisons of airfoils.

airfoils at different angles of attack (Figure 13), it is seen that the C_L values reach their maximum value at 11°. In this study, the maximum angle of attack required in the system does not exceed 10°. Although the C_L value of the NACA 63-412 airfoil is lower than NACA 6412, its performance is higher because of its lower C_D value.

3.2. Comparison of Existing Fan and New Fan

Considering the catalogue values (Table 1), the axial fan currently used in a real underground mining operation is expected to provide a flow rate of 2.87 kg/s between 3700-4700 rpm. According to CFD analyses (Table 6), the existing fan reaches a flow rate of 2.87 kg/s at a speed of 4700 rpm between these speeds. When the CFD analysis results of the new fan created with the fan blade designed using the NACA 63-412 airfoil, which shows the highest performance (Table 6), it is seen that it can provide a flow rate of 2.87 kg/s with a speed of 3700 rpm. Figure 14 and Figure 15 show that the desired flow rate and pressure differential can be achieved at lower speeds with the new

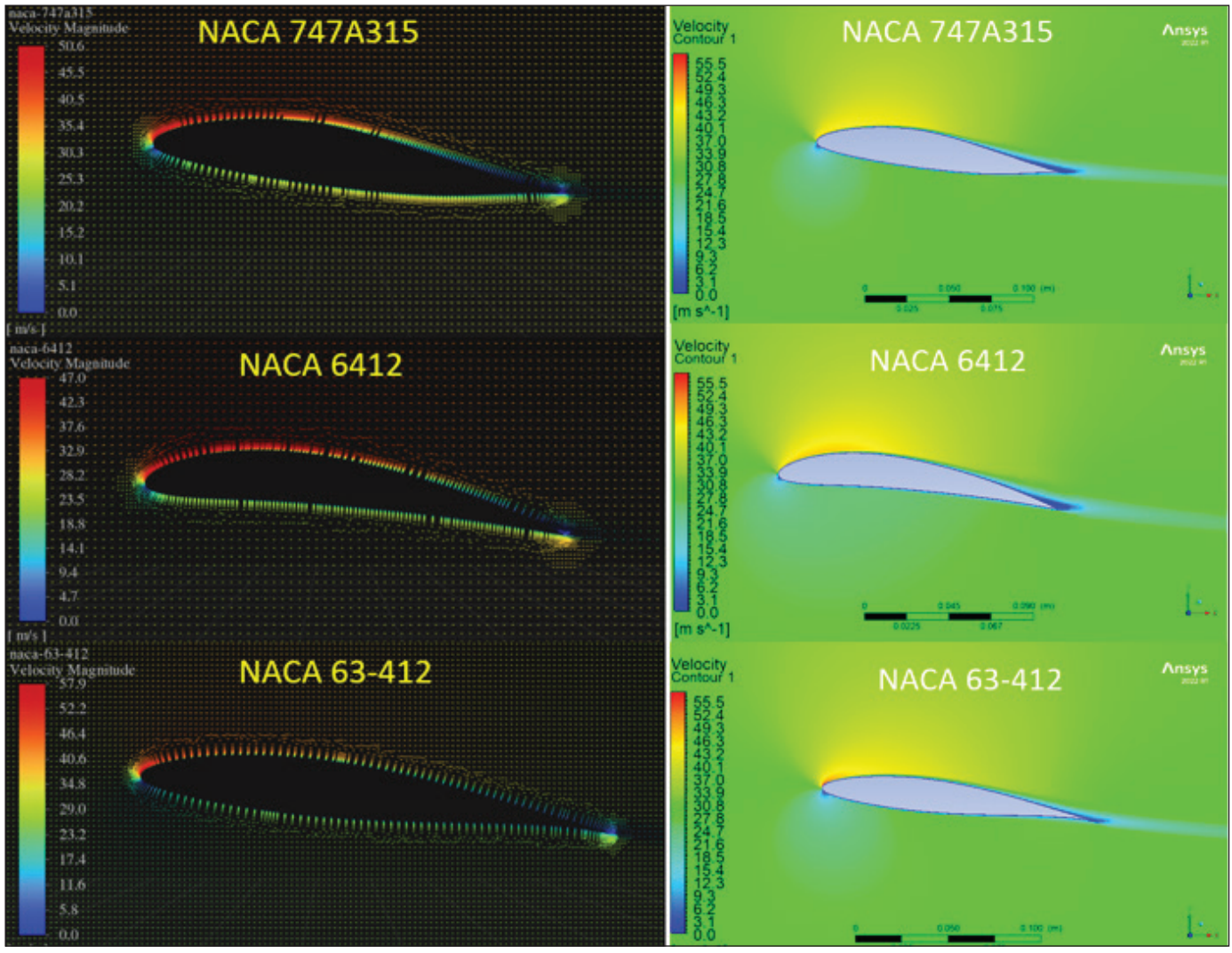

Figure 12. Velocity vectors and velocity contours of the wing blades.

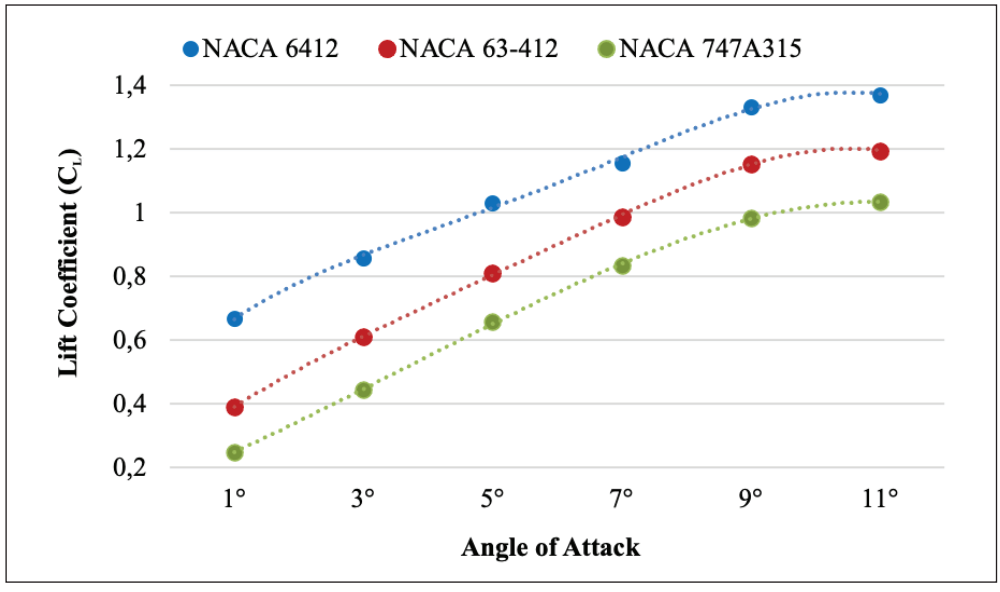

Figure 13. Comparison of values of airfoils at different angles of attack.

Table 6. CFD analysis results of the existing and new fan in the range of 3700-4700 rpm.

Number of revolutions (n) (rev/min)	Current Fan		New Fan	
	Mass Flow ($\dot{m}$) (kg/s)	Total Pressure Difference (ΔP) (Pa)	Mass Flow ($\dot{m}$) (kg/s)	Total Pressure Difference (ΔP) (Pa)
3700	1	347	1	503
3700	1.5	328	2.3	333
3700	2*	176	2.5*	221
4000	2*	275	2	685
4000	2.2	189	2.5	383
4000	2.4	81	2.75*	233
4700	2*	511	2.5	834
4700	2.5	312	2.75	649
4700	2.75	163	2.87*	580

* The results obtained in the new design at constant mass flow rate and different rotational speeds of the existing fan shows the mass flow rate values.

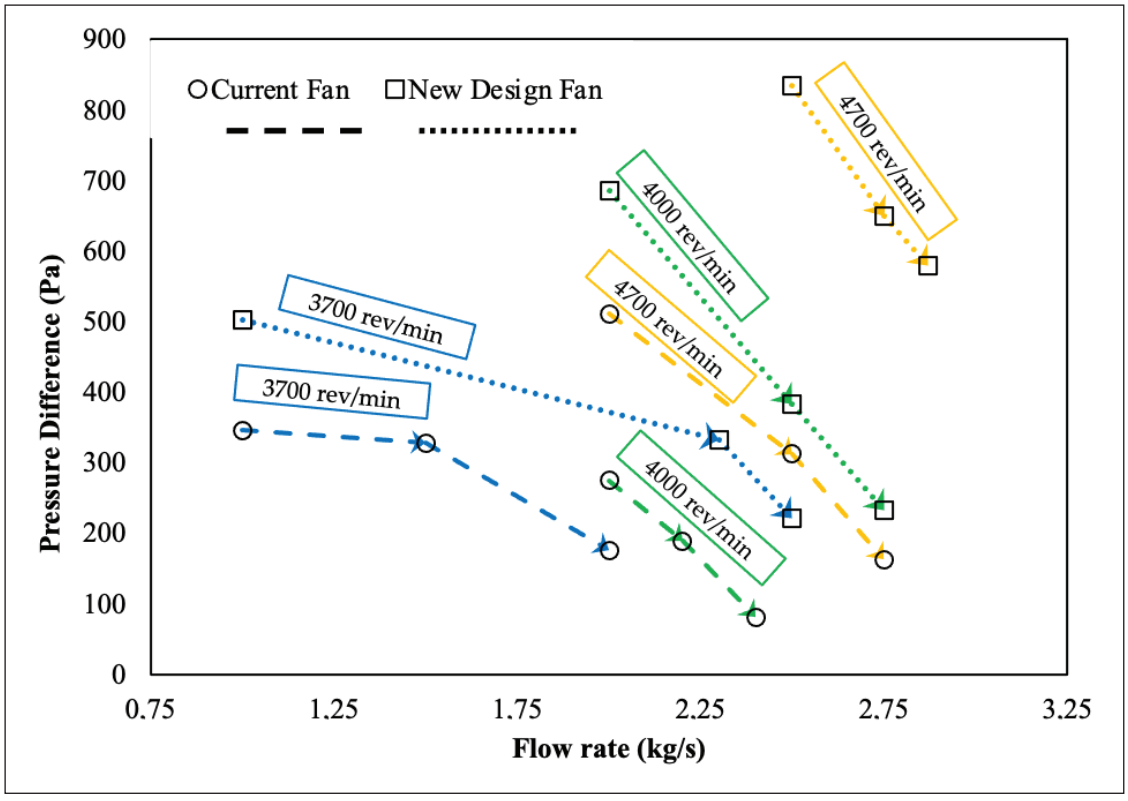

Figure 14. Flow-pressure graph of the existing fan and the new fan at 3700-4700 rpm.

fan, which can pump a flow rate of 2.87 kg/s at 4700 rpm with a pressure difference of 580 Pa, and its performance superiority over the existing fan.

At 4000 rpm-2 kg/s operating conditions, the flow rate of the new fan increased between 25%-435% compared to the existing fan (Table 7).

4. Conclusion and Suggestions

In this study, in order to increase the efficiency of the fan used in the ventilation of a real underground mining operation, a new blade profile that can be an alternative to the blades recommended to be used in underground mine fan blades in the literature is pro-posed A new rotor blade was designed

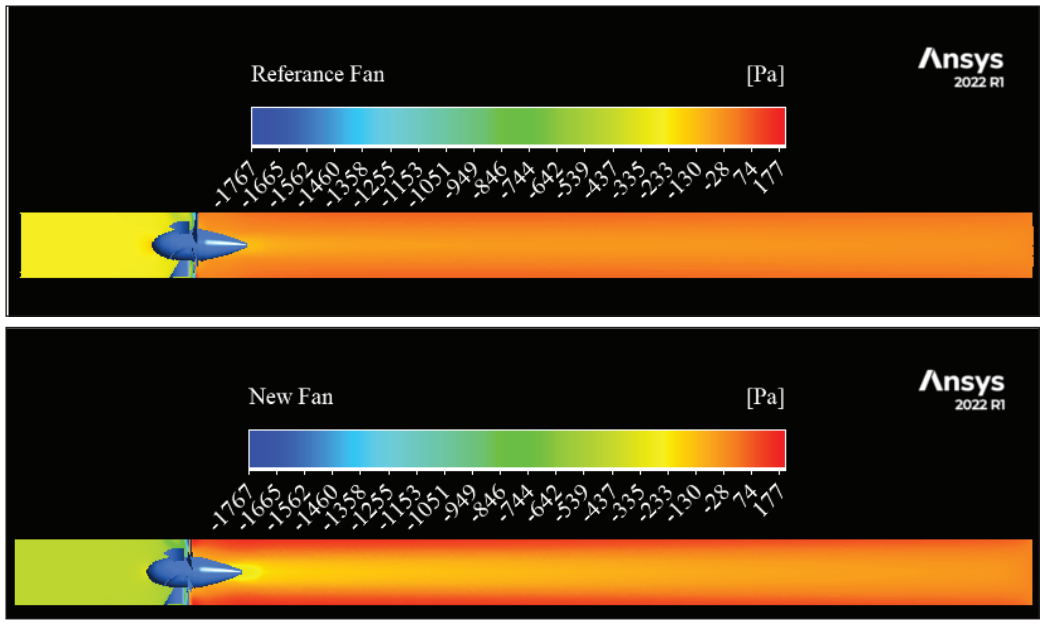

Figure 15. Comparison of the pressure contours of the existing fan and the new fan at 4000 rpm and 2 kg/s flow rate.

Table 7. Improvement in the constant flow rate value in the range of 3700-4700 rpm for the existing fan.

Number of revolutions (n) (rev/min)	Current Fan		New Fan		Increase (%)
	Mass Flow ($\dot{m}$) (kg/s)	Total Pressure Difference (ΔP) (Pa)	Mass Flow ($\dot{m}$) (kg/s)	Total Pressure Difference (ΔP_t) (Pa)	
3700	2	176	2.5	221	25.00%
4000	2	275	2.75	233	37.50%
4700	2	511	2.87	489	43.50%

with the profile with the highest performance and the results of CFD analyses of the reference fan and the new fan were compared with each other. According to the results of CFD analyses performed with NACA 747A315, NACA 6412 and NACA 63-412, NACA 63-412 has the highest wing performance ratio. NACA 6412 performed better than NACA 747A315, confirming the work of Hassen (2021).

In order to see the change in flow rate and pressure difference of NACA 63-412 in the existing fan, CFD analyses of the new fan, which was designed by adhering to the geo-metrical characteristics of the fan, showed that the new fan reached higher flow rates at the same pressure difference at 3700-4700 rpm. Under 4000 rpm-2 kg/s operating conditions, the flow rate of the new fan increased between 25% and 43.5% compared to the existing fan.

In this study, the improved fan was designed to provide the flow rate (2.87 kg/s) specified in the technical catalogue of the product at the desired pressure difference (330 Pa) and at the lowest possible speed (3700 rpm), but it was observed that the new fan was slightly below these requirements. It is thought that the reason for this is related to the stator geometry and blade angles and that studies on this fan should continue with the stator part of the fan.

Author contribution: Conceptualization, Güneyhan Taşkaya (G.T.) and Beytullah Erdoğan (B.E.); methodology, G.T. and B.E.; software, G.T.; validation, G.T.; formal analysis, G.T.; investigation, G.T. and B.E.; resources, G.T. and B.E.; data curation, G.T. and B.E.; writing-original draft preparation, G.T., B.E. and G.T.; writing-review and editing, G.T., B.E.; visualization, G.T.; supervision, B.E. All authors have read and agreed to the published version of the manuscript.

Nomenclature	
F_L	Buoyancy Force (N)
F_D	Drag Force (N)
C_L	Lift Coefficient
C_D	Drag Coefficient
C_L/C_D	Performance Ratio
ρ	Density (kg/m^3)
V_a	Axial Velocity (m/s)
Q	Volumetric Flow Rate (m^3/s)
ΔP_t	Total Pressure Difference (Pa)
μ	Dynamic Viscosity (Pa.s)
c	Chord Length (m)
s	Pitch Distance (m)
β_1	Wing Entry Angle
β**m**	Avarege Wing Angle
β_2	Wing Exit Angle
W_1	Entery Relative Flow Velocity (m/s)
Wm	Average Relative Flow Velocity (m/s)
W_2	Exit Relative Flow Velocity (m/s)
U	Tangential Velocity (m/s)
V_{2u}	Absolute Velocity (m/s)
η	Hydraulic Efficiency
$\dot{m}$	Mass Flow Rate (kg/s)
τ	Tork (Nm)
$W_{shaft,power}$	Shaft Power (kW)
σ	Solidity
t	Time (s)
u	Velocity Vector (m/s)
i	The velocity (x) Component (m/s)
j	The velocity (y) Component (m/s)
x	Position Vector (m)
S	Discretisation Term
n	Number Of Revolutions (rev/min)
w	Angular Velocity (m/s)

5. References

Bacak, A. 2016. Experimental and numerical analysis of axial fan performance analysed by methods. MSc Thesis, Department of Mechanical Engineering, Gebze Technical University, 57 s.

Bakhtar, H., Alsahafi, N., Almehmadi, M. et al. 2024.Flow-induced noise and vibration in axial fan: a case study. Journal of Umm Al-Qura University for Engineering and Architecture.1, 1-18, Doi:10.1007/s43995-024-00079-9

Castegnaro, SA. 2017. Critical Analysis of the Differences Among Design Methods for Low-Speed Axial Fans. Proceedings of the ASME Turbo Expo., 26-30, USA. Doi: 10.1115/GT2017-64276

Çakır, ET. 2018. Effects of rotor-stator interaction surface modelling and shifting of airfoils on the performance of axial fans. MSc Thesis, Department of Mechanical Engineering, Istanbul Technical University, 97 s.

Çengel, YA., Cimbala, JM. 2018. Fluid Mechanics, Fundamental and Applications, Turbomachinery (4th ed). McGraw-Hill, New York, 825-827 pp.

Çoban, M. 2019. Flow separation on an airfoil on a wing control by opening gap. MSc Thesis, Department of Mechanical Engineering, Sivas Cumhuriyet University, 126 s.

Dilmaç, E. 2019. Naca 4415 wind turbine blade the effect of the edge of the fingertip on the profile analysis. MSc Thesis, Department of Mechanical Engineering, Konya Technical University, 99 s.

Drwiega, A., Szelka, M., Turewicz, A. 2019. Improvement of auxiliary ventilation efficiency in underground workings. IOP Con-ference Series: Earth and Environmental Science, 261(1). Doi:10.1088/1755-1315/261/1/012007.

Fakhari, SM., Mrad, H. 2024. Optimization of an axial-flow mine ventilation fan based on effects of design parameters. Results in Eng. 21, 101662. Doi:10.1016/j.rineng.2023.101662.

Fan, C., Adjei, AR., Wu, Y., Wang, A. 2020. Parametric study on the aerodynamic performance of a ducted-fan rotor using free-form method. Aerospace Science and Technology. 101, 105842. Doi:10.1016/j.ast.2020.105842.

Fernando, VN., Mudunkotuwa, DY. 2021. Bio-Inspired Aircraft Wing Modification Analysis in ANSYS Fluent. 10th International Conference on Information and Automation for Sustainability, Negambo, Sri Lanka, 11-13. Doi:10.1109/ICIAfS52090.2021.9605821

Galpin, P., Hansen, T., Scheuerer, G., Kelly, R., Hickman, A., Jemcov, A., Morris, SC. 2017. Validation of transonic axial compressor stage unsteady state rotor-stator simulations. Proceedings of the ASME Turbo Expo, 26-30, USA,

Hassen, AE. 2021. Flow characterization in mine ventilation fan blade design using CFD. Journal of Sustainable Mining. 20, 144–156. Doi:10.46873/2300-3960.1063.

İlikan, NA. 2014. Blade profile arrangement of axial fans effects on performance. PhD Thesis, Department of Mechanical Engineering, Istanbul Technical University, 212 s.

Jung, JH., Joo, WG. 2019. The effect of the entrance hub geometry on the efficiency in an axial flow fan. Intern. Journal of Refrigeration. 101, 90-97. Doi:10.1016/j.ijrefrig.2019.02.026.

Keklikoğlu, ÖH. 2019. Design, construction and performance evaluation of axial flow fans. MSc Thesis, Department of Mechanical Engineering, Middle East Technical University, 127 s.

Kong, C., Wang, M., Jin, T. et al. 2023. The blade shape optimization of a low-pressure axial fan using the surrogate-based multi-objective optimization method. Journal of Mechanical Science and Technology. 37, 179–189. Doi:10.1007/s12206-022-1219-y.

Korkmaz, Ü. 2018. Adjustable wing design to delay stall. MSc Thesis, Aircraft and Aerospacing Engineering, Gaziantep University, 51 s.

Köse, Ö. 2018. Axial gas turbines wing parameters analysis. MSc Thesis, Mechanical Engineering Department, Iskenderun Technical University, 76 s.

Krasyuk, AM., Kosykh, PV. 2023. Aerodynamic Design of Axial Fan with Guide Vane for Reverse Air Flow. Journal of Mining Science. 59, 424-432. Doi:10.1134/S1062739123030092.

Luo, D., Huang, D., Sun, X., Chen, X., Zheng, ZA. 2017. Computational Study on the Performance Improvement of Low-Speed Axial Flow Fans with Microplates. Journal Applied Fluid Mechanics. 10, 1735-3645. Doi:10.29252/JAFM.73.245.27492.

Panigrahi, DC., Mishra, DP. 2014. CFD Simulations for the Selection of an Appropriate Blade Profile for Improving Energy Efficiency in Axial Flow Mine Ventilation Fans. Journal of Sustainable Mining. 13, 15-21. Doi:10.7424/jsm140104.

Park, K., Choi, H., Choi, S., Sa, Y. 2019. Effect of a casing fence on the tip-leakage flow of an axial flow fan. International Journal of Heat and Fluid Flow. 77, 157-170. Doi:10.1016/j.ijheatfluidflow.2019.04.005.

Tonello, N., Eudel, Y., Meux, L., Ferrand, M. 2017. Frozen Rotor and Sliding Mesh Models Applied to the 3D Simulation of the Francis 99 Tokke Turbine with Code Saturne. Journal of Physics Conference Series. 782, 012009. Doi:10.1088/1742-6596/782/1/01200.

Yılmaz, M., Köten, H., Çetinkaya, E., Coşar, ZA. 2018. A Comparative CFD analysis of NACA0012 and NACA4412 airfoils. Journal of Energy Systems. 2, 145–159. Doi:10.30521/jes.454193.